

## ORIGINAL ARTICLE



# Real-time auto-segmentation of the ureter in video sequences of gynaecological laparoscopic surgery

Zhixiang Wang<sup>1,2</sup>  | Chongdong Liu<sup>3</sup> | Zhen Zhang<sup>2,4</sup> | Yupeng Deng<sup>3</sup> | Meizhu Xiao<sup>3</sup> | Zhiqiang Zhang<sup>3</sup> | Andre Dekker<sup>2</sup> | Shuzhen Wang<sup>3</sup> | Yujiang Liu<sup>1</sup> | LinXue Qian<sup>1</sup> | Zhenyu Zhang<sup>3</sup> | Alberto Traverso<sup>2</sup> | Ying Feng<sup>1</sup>

<sup>1</sup>Department of Ultrasound, Beijing Friendship Hospital, Capital Medical University, Beijing, China

<sup>2</sup>Department of Radiation Oncology (Maastr), GROW-School for Oncology, Maastricht University Medical Centre+, Maastricht, The Netherlands

<sup>3</sup>Department of Obstetrics and Gynecology, Beijing Chao-Yang Hospital, Capital Medical University, Beijing, China

<sup>4</sup>Zhejiang Cancer Hospital, Institute of Basic Medicine and Cancer (IBMC), Chinese Academy of Sciences, Hangzhou, Zhejiang, China

## Correspondence

Alberto Traverso and Ying Feng.  
Email: [alberto.traverso@maastro.nl](mailto:alberto.traverso@maastro.nl) and [15116988424@163.com](mailto:15116988424@163.com)

## Abstract

**Background:** Ureteral injury is common during gynaecological laparoscopic surgery. Real-time auto-segmentation can assist gynaecologists in identifying the ureter and reduce intraoperative injury risk.

**Methods:** A deep learning segmentation model was crafted for ureter recognition in surgical videos, utilising 3368 frames from 11 laparoscopic surgeries. Class activation maps enhanced the model's interpretability, showing its areas. The model's clinical relevance was validated through an End-User Turing test and verified by three gynaecological surgeons.

**Results:** The model registered a Dice score of 0.86, a Hausdorff 95 distance of 22.60, and processed images in 0.008 s on average. In complex surgeries, it pinpointed the ureter's position in real-time. Fifty five surgeons across eight institutions found the model's accuracy, specificity, and sensitivity comparable to human performance. Yet, artificial intelligence experience influenced some subjective ratings.

**Conclusions:** The model offers precise real-time ureter segmentation in laparoscopic surgery and can be a significant tool for gynaecologists to mitigate ureteral injuries.

## KEYWORDS

gynaecological laparoscopic surgery, segmentation, surgical video, ureter

## 1 | INTRODUCTION

Compared with traditional laparotomy, gynaecological laparoscopic surgery has been shown to result in fewer incidences of bleeding, fever, and infection, as well as shorter hospital stays, a faster return to normal activities, and an improved long-term quality of life, earning it recognition for its minimal invasiveness.<sup>1-3</sup> A study

conducted in 2014 found that total laparoscopic hysterectomy (THL) significantly enhances the perioperative outcome of patients with endometrial cancer, decreases the reoperation rate, and reduces postoperative complications when compared to laparotomy.<sup>4</sup> However, ureteral injuries frequently occur during gynaecologic laparoscopic surgery when performing operations to separate the parametric tissue from the uterus. It is challenging to separate the

Zhixiang Wang and Chongdong Liu have contributed equally to this work and share the first authorship.

Alberto Traverso and Ying Feng have contributed equally to this work and share the corresponding authorship.



uterine artery and ureter, and this must be carefully performed along the ureteral tunnel, where ureteral injuries are due to the complex and obscured anatomy.<sup>5,6</sup>

In women, the ureter lies medial to the infundibulopelvic ligament, then traverses the broad ligament of the uterus, passes below the uterine artery (approximately 2 cm), courses through the cervix, and enters the bladder. Ureteral damage can occur during surgery on adjacent anatomical structures.<sup>7</sup> Such injuries are reported in 1.3 per 1000 cases of abdominal hysterectomy, 0.2 per 1000 cases of vaginal hysterectomy, and 13–42 per 1000 cases of radical hysterectomy.<sup>8–11</sup> Ureteral injuries are more common during TLH, and they are frequent and most studies report <1% of injuries. It usually occurs near the cardinal ligament where the ureter is close to the uterine artery.<sup>7,8</sup> Fujii recommended lifting the uterine artery and carefully separating the ureter and the uterine artery.<sup>12</sup> Kobayashi proposed the water separation techniques.<sup>13</sup> However, implementing these procedures is not easy.

Traditionally, texture-based methods were utilised for segmenting organs and tissues in surgical videos or images.<sup>14</sup> Recently, deep learning (DL) methods, have emerged as promising alternatives,<sup>15</sup> offering enhanced classification performance in surgery. B. Harangi et al. proposed a ureter and uterine artery classification model,<sup>16</sup> yet real-time imaging has not been extensively studied. Real-time segmentation of the ureter, without the need for additional fluorescent agents during gynaecological laparoscopic surgery still requires further exploration. Time requirements for surgery are stringent, and delays can endanger the patient's life. The model's

real-time performance must be under 42 ms per frame.<sup>17</sup> Beyond the identification and separation of the ureter, recognising its boundaries to help avoid thermal injury is also of crucial importance, further justifying the need for this technology.

Beyond the identification and separation of the ureter, recognising its boundaries to help avoid thermal injury is also of crucial importance, further justifying the need for this technology. There are only a few studies that demonstrate the real-world clinical impact and principles of artificial intelligence (AI) segmentation methods.<sup>16,18</sup>

Therefore, in this study, we aim to develop a real-time interpretable AI application that can perform segmentation of the ureter with sufficient accuracy during laparoscopic hysterectomy.

## 2 | MATERIALS AND METHODS

To demonstrate the clinical applicability of the proposed method, we adopted a multi-faceted approach. Initially, the dataset was collated and subjected to image pre-processing. Subsequently, the model's accuracy and speed were assessed using an objective (Dice coefficient, Hausdorff 95 distance, and time consumption). The clinical potential was further substantiated through a subjective methodology (End-User Investigation). To elucidate the model's functionality, visualisation techniques such as feature maps, and class activation maps (CAM) were employed. The entire workflow is depicted Figure 1.

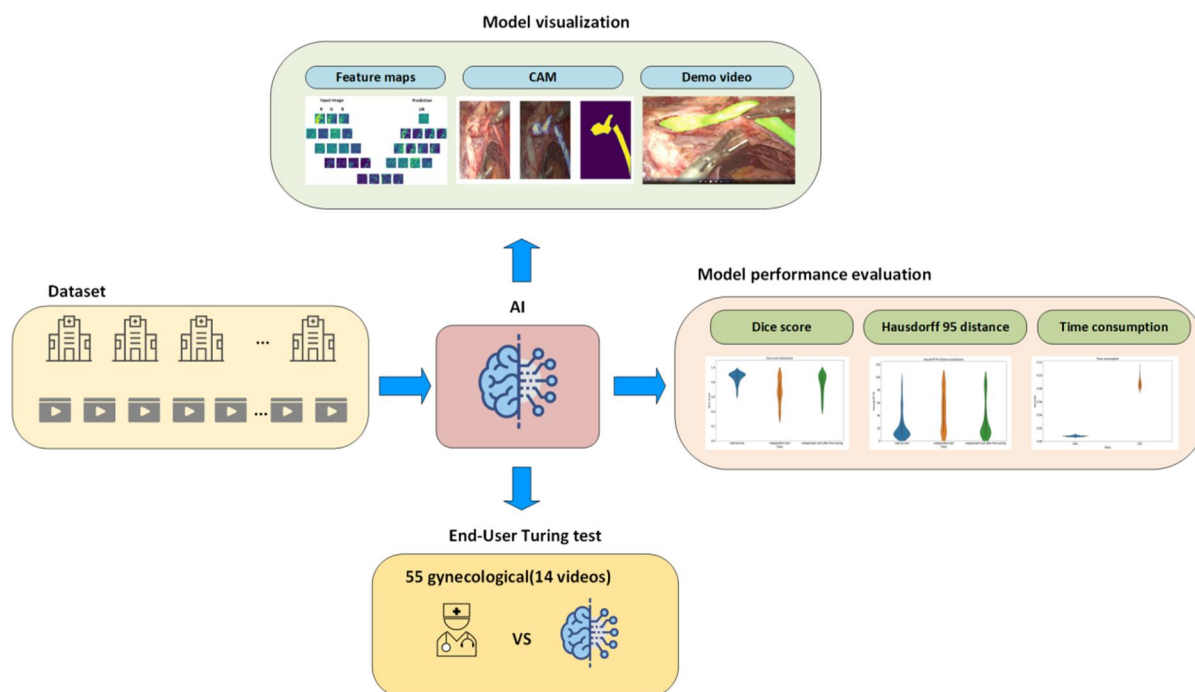


**FIGURE 1** The workflow of the experiment. The model was trained in the dataset. Then, the model performance evaluation methods and end-user investigation were applied. Moreover, the model visualisation methods including the feature maps and the class activation map (CAM) were used.



## 2.1 | Patients

A cohort of 3368 frames at a rate of one frame per second was retrospectively compiled from 11 surgical videos, emphasising instances where the ureter was distinctly visible, such as a complete view of the pelvic sidewalls, were retrospectively extracted from 11 surgical video records. Ten videos were designated as the training dataset, which was randomly split into a training set and an internal test set at a 7:3 ratio, and the remaining video constituted the external independent test set. The surgeries comprised two standard laparoscopic hysterectomies, six laparoscopic hysterectomy + lymphadenectomy, and three laparoscopic endometriosis lesion resections (deeply infiltrating endometriosis). All these patients showed the presence of adhesions, and the average BMI was 28.5. These procedures were conducted by seasoned gynaecological oncology experts at Beijing Chaoyang Hospital, each with over 20 years of experience. The research received ethical approval from the review committee of Beijing Chaoyang Hospital, Capital Medical University.

## 2.2 | Image pre-processing

To mitigate the variability in the image colour due to differing illumination conditions, scene and the hardware, standardisation and resizing techniques were applied. Details are provided in Supporting Information S1.

## 2.3 | Reference standard

Three gynaecologists, each with approximately 6 years of laparoscopic expertise, annotated the images. Uterine delineation was verified against intraoperative findings and surgical video records. Cross-validation among the annotators was performed, and discrepancies or uncertainties (seven images) were resolved through discussion or consultation with additional experienced colleagues. This consensus served as the gold standard for our dataset.

## 2.4 | Deep learning architecture

The UNet was applied as the DL model (shown in Figure 2A), because it is widely used in clinical segmentation tasks.<sup>19</sup> It is composed of an encoder, a decoder, and a skip connection module. Our source code can be found here: [[https://gitlab.com/UM-CDS/Surgical\\_video\\_segmentation](https://gitlab.com/UM-CDS/Surgical_video_segmentation)]. The details of the model structure and training strategy along with the loss function are given in Supporting Information S1.

## 2.5 | Model performance evaluation

The robustness of the model, particularly after fine-tuning, was appraised on both the internal and independent test sets using the Dice coefficient, Hausdorff 95 distance, and time consumption metrics on graphics processing unit (GPU) and central processing unit (CPU) platforms. Evaluation methodologies are elaborated in Supporting Information S1.

## 2.6 | End-user investigation

While AI tasks conventionally depend on objective metrics like accuracy, Dice and area under curve. But for clinical tasks, objective measures alone may not be enough to meet clinical requirements. For physician-oriented AI, the model's assistant ability and acceptance of clinical needs are to be considered. To evaluate whether the DL-based segmentation is helpful for gynaecological surgeons during laparoscopic surgery, 55 gynaecological surgeons with different levels of expertise (director, assistant director, attending and resident) from eight different regions (Xi'an, Hangzhou, Lanzhou, Yangzhou, Ningxia, Changzhou, Xianyang, Anshun) in China were asked to perform the blinded investigation. The details of the investigation are illustrated in Supporting Information S1.

During the investigation, the gynaecologist watched the video and after that answered the questionnaire (Supporting Information S1). Besides this, subjective comments about the DL segmentation method were also collected.

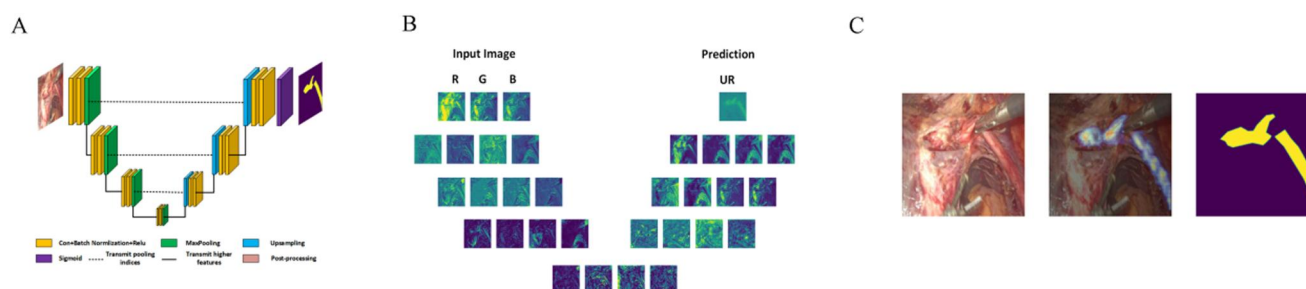


**FIGURE 2** The AI model structure and visualisation methods. (A) the structure of the UNet model. (B) the feature maps in each convolution block. (C) The class activation map on the output layer. AI, artificial intelligence.



Statistical analyses were conducted using IBM SPSS 23.0, employing the Mann–Whitney *U* test for two-group comparisons and the Kruskal–Wallis Test for multiple-group analyses, given the data's non-normal distribution.

## 2.7 | AI model visualisation

Feature maps and the CAM methods were implemented for model visualisation to illustrate the image transformation process and to highlight areas of 'DL model attention', respectively. The visualisation techniques are described in Supporting Information S1.

## 2.8 | Dynamic real-time segmentation

A dynamic demonstration video (Video S1) showcases the model's ability to delineate in real-time during intricate surgical procedures, obviating the need for additional materials such as fluorescence specialised glasses.

## 3 | RESULTS

All patients in this study exhibited adhesions, with an average body mass index (BMI) of 28.5. During the surgical procedures, meticulous attention was given to achieving a clear visualisation of the pelvic sidewalls with a focus on the ureter. The sidewall was methodically opened, and the ureter was thoroughly dissected.

### 3.1 | Segmentation performance

The distributions of the Dice score, Hausdorff 95 distance and time consumption are illustrated in Figure 3A–C, respectively.

The mean Dice score was 0.86 (95% confidence interval [CI]: 0.64–0.95), 0.67 (95% CI: 0.33–0.93) for the independent test set prior to fine-tuning, and 0.77 (95% CI: 0.46–0.95) after fine-tuning, respectively. The mean Hausdorff 95 distance is 22.60 (95% CI: 4.68–82.85), 47.36 (95% CI: 8.95–97.82) and 32.96 (95% CI: 6.22–96.95) on the internal set and independent test set before and after fine-

tuning, respectively. The mean time consumption of each frame in GPU and CPU were 0.008 s (95% CI: 0.007–0.01) and 0.0873 s (95% CI: 0.080–0.10), respectively.

## 3.2 | End-user investigation results

### 3.2.1 | Basic information for gynaecologists

The gynaecologists' experience ranged from 4 to 28 years, with an average of 15 years (the distribution of work year experience is presented in Supporting Information S1: Figure 1). Their primary areas of expertise were gynaecological oncology and laparoscopic surgery. Their specialised experience in particular diseases varied from 2 to 28 years, averaging 8 years. Figure 4, which comprises 12 subjective questions (A–L, Supporting Information S1), captures the gynaecologists' perceptions of DL in healthcare. Currently, their exposure to DL in clinical practice and surgical procedures is relatively limited. Nonetheless, they exhibited a high level of trust and expectation in DL-enhanced medical care.

No significant differences were observed in the rated accuracy ( $p = 0.932$ ), specificity ( $p = 0.805$ ), and sensitivity ( $p = 0.676$ ) when comparing DL-assisted evaluations with those performed by gynaecologists (refer to Figure 5A–C). The task of recognising and segmenting the ureter during the gynaecological laparoscopic surgery was acknowledged as a challenging task (Figure 5D).

Furthermore, there was no significant difference between the DL-segmented and gynaecologist-labelled ureters (Figure 5E,F). The majority of gynaecologists concurred that the DL model holds significant practical and clinical applicability, whether for training purposes or during laparoscopic surgeries.

To depict the varying perspectives on AI in healthcare among gynaecologists at different professional levels, group statistics were employed on the basis of experience. As shown in Figure 6, among the 12 subjective questions, the score of question 2 (Q2, do you have prior experience with any AI in the clinic? Supporting Information S1) ( $p = 0.027$ ) and question 3 (Q3, do you conduct AI research?) ( $p = 0.017$ ) indicated a statistically significant difference, the directors are the group who has the most experience with AI. (The remaining pie charts are shown in Supporting Information S1: Figure 2).

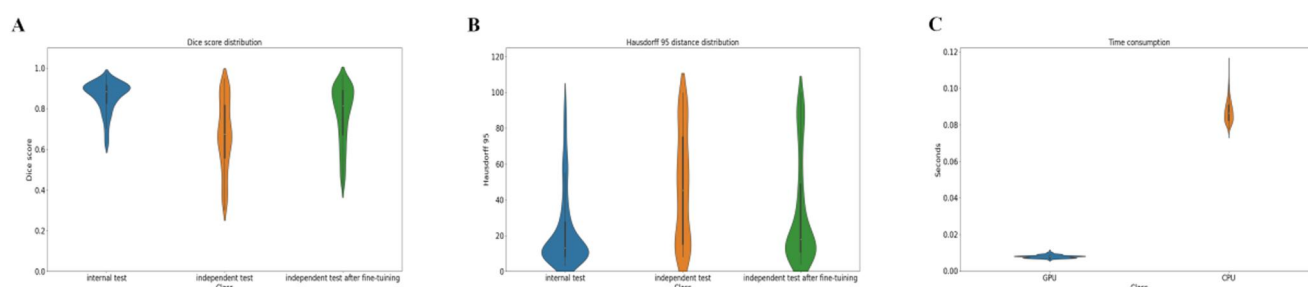
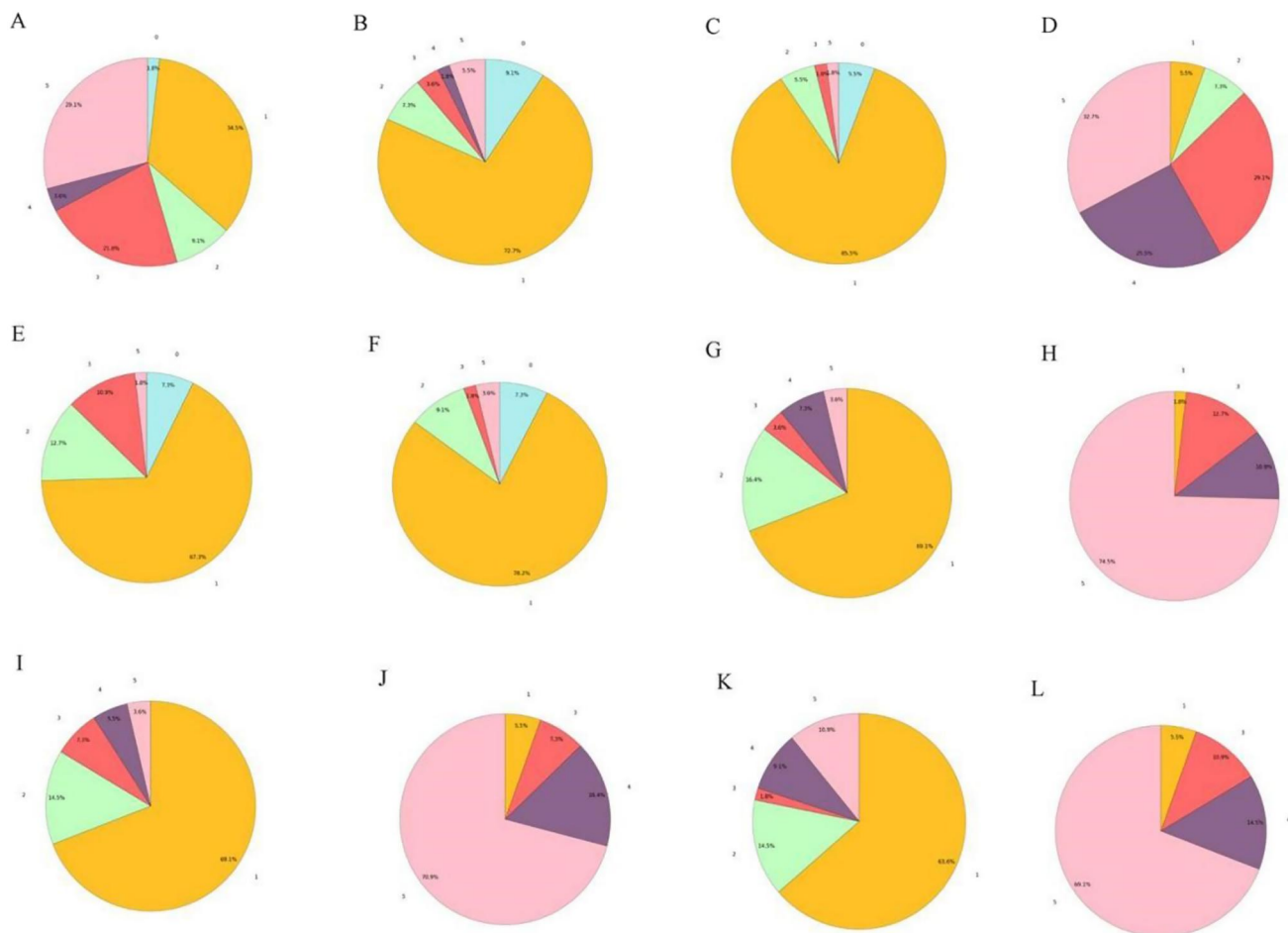
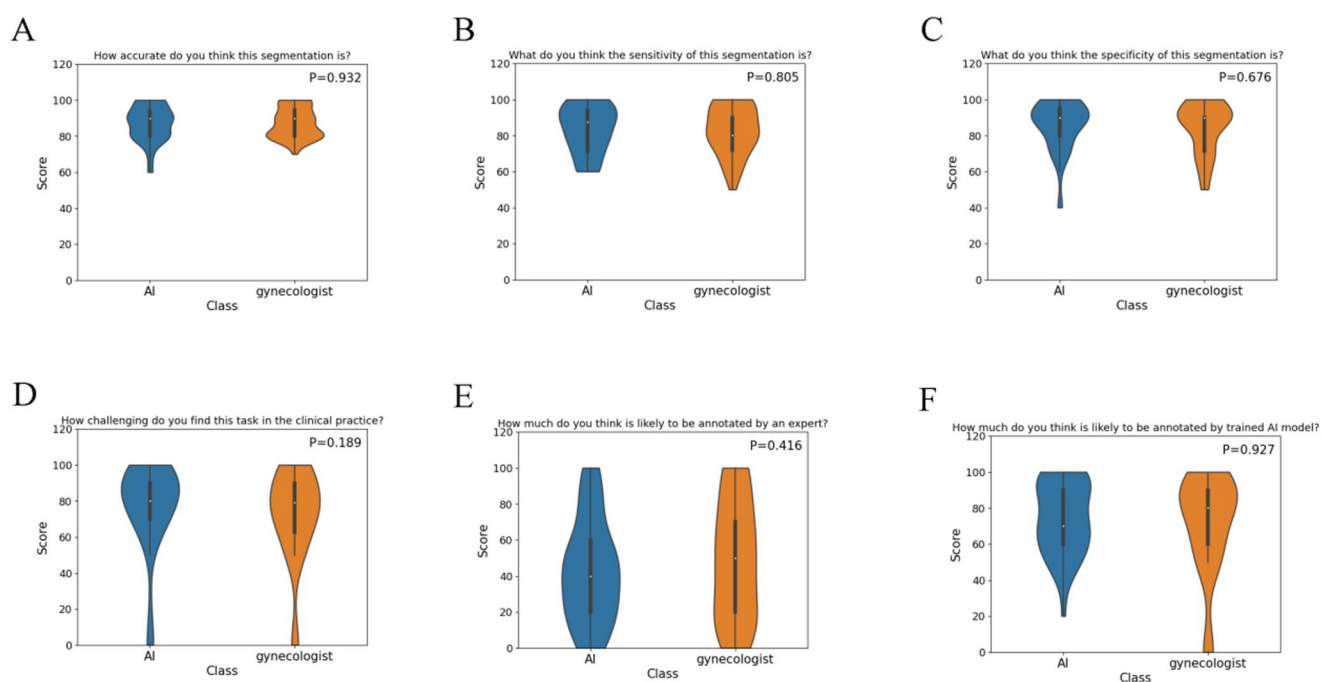


FIGURE 3 The Dice score distribution (A) the Haus95 distribution (B) and the time consumption (C) in the test set.



**FIGURE 4** The perspectives of a gynaecologist on AI in healthcare. A-L represent the 12 questions (Supplementary F) from front to back in order. AI, artificial intelligence.



**FIGURE 5** Distribution of quantitative Turning test outcomes by gynaecologists. The terms AI and gynaecologists mean the video was annotated by AI and gynaecologists, respectively. AI, artificial intelligence.



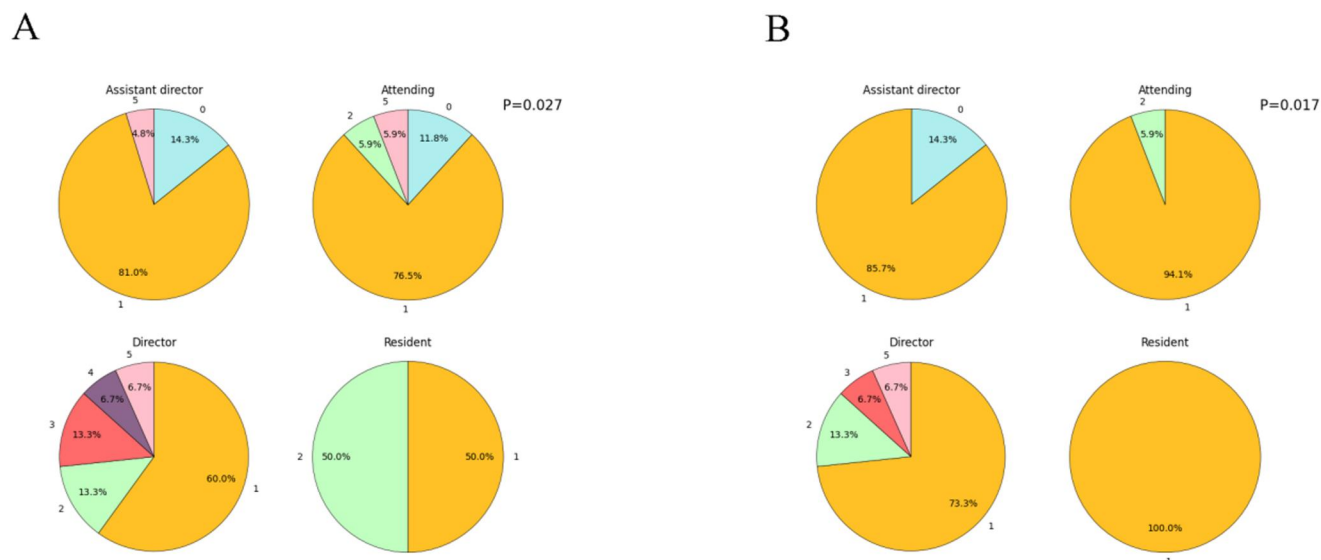


**FIGURE 6** The difference between the positions of gynaecologists about the experience with AI. (A) the answers of question 2 (Q2, do you have prior experience with any AI in clinic? 1 = none, 5 = a lot). (B) The answers to question 3 (Q3, do you conduct AI research? 1 = none, 5 = a lot). The colour legends are listed below: 1-yellow, 2-green, 3-red, 4-purple, 5-pink. AI, artificial intelligence.

### 3.3 | Activation and feature maps

The feature map corresponding to the convolutional layer's activity during the ureter segmentation process is presented in Figure 2B. The surgical video image was divided into three red ®, green ®, and blue ® channels as inputs and passed through the convolutional layer. With the encoding process, a large amount of information is compressed, and the feature map becomes abstract due to the arithmetic components of the convolutional layer. The network's output, displaying the prediction result, is revealed at the culmination of the decoding phase.

As depicted in Figure 2C, from the CAM images demonstrate that the DL model pays heightened attention to the ureter's site and adjacent blood vessels.

## 4 | DISCUSSION

In gynaecological surgery, the manipulation of the ureter tunnel frequently results in inadvertent ureteral injuries.<sup>6</sup> To prevent such damage, precise handling of the ureter is crucial. Several techniques to mitigate ureteral injury have been reported by surgeons.<sup>12,13,20,21</sup> The precise recognition of the anatomy of the ureter is important in gynaecological surgery. Fujii recommended lifting the uterine artery and carefully separating the ureter and the uterine artery.<sup>12</sup> Kobayashi proposed the water separation techniques.<sup>13</sup> However, implementing these procedures is not easy. It is challenging to separate the uterine artery and ureter, and this must be carefully performed along the ureteral tunnel, where ureteral injuries and massive bleeding often occur because of the blinded and complex

anatomy.<sup>5,6</sup> B. Harangi et al. proposed a classification model that can classify the ureter and uterine artery images.<sup>16</sup> However, this semi-automatic method requires manual marking on static images and does not support real-time segmentation and guidance during surgery. In this study, we developed a DL model that can perform the real-time segmentation of the ureter during gynaecological laparoscopic surgery.

To evaluate the model, first, the Dice score, Haus95 and time consumption were used to evaluate the DL performance in an independent test set in both GPU and CPU. Second, the end-user investigation was performed by 55 gynaecological surgeons at four different positions (director, assistant director, attending, and resident) from eight different regions in China who evaluated the segmentation performance (accuracy, sensitivity, specificity, probability of gynaecologist annotation etc.). Additionally, the feature maps and CAM were used to visualise the rationale behind AI decisions.

To ascertain the robustness of our model, we evaluated its performance on a curated collection of 11 gynaecological laparoscopic surgery videos, each depicting varied operational techniques and anatomical sites.

The network's efficacy was reflected in a Dice coefficient nearing 0.9 and most Hausdorff 95 distances falling below 25, signifying the model's adeptness in precisely mapping the ureter's contours and location. Such precision plays a crucial role in enhancing operational procedures and mitigating the risk of ureteral injuries during gynaecological laparoscopic surgery. Nevertheless, the heterogeneity inherent in surgical practices—owing to disease-specific and intra-operative variations—can lead to a notable decline in predictive accuracy, as evidenced by the drop from a Dice score of 0.86 to 0.67 in previously unseen surgical fields. This decline could be indicative of



data overfitting. However, subsequent fine-tuning improved the model's performance, with a 10% enhancement in the Dice score, demonstrating that targeted adjustments using similar field frames can substantially refine the model's efficacy for particular datasets, thereby addressing the issue of robustness.

Taking into account the safety and timeliness requirements of clinical surgery, the DL model needs to have the ability to perform real-time segmentation during surgery. In a real-time task, the time consumption for each frame should be less than 42 ms.<sup>22</sup> The time consumption of this model is 8 and 87 ms per frame on GPU and CPU, respectively. As also shown in Video S1, our model can dynamically segment the ureter in real-time without the need for special subsidiary materials such as fluorescence and glasses.<sup>23</sup>

From the investigation results, there were no significant differences between the DL-segmented and gynaecologist-labelled ureters. Recognition and segmentation of the ureter during the gynaecological laparoscopic surgery were generally considered to be a challenging task. We noted that the most experienced physician (the director has the most DL experience, but that the clinical application of DL in surgery is still uncommon).

Gynaecologists attest that this DL innovation is a beneficial tool, aiding in the preservation of vital tissues and blood vessels during surgery. It provides an intuitive and lucid anatomical view, ensuring that the ureter is clearly visible, potentially preventing ureteral injury and consequent complications. This enhancement in surgical precision and safety, coupled with the potential to address medical resource scarcity, underlines the model's significant clinical potential and value, particularly in complex cases where ureteral visibility is compromised. For less experienced surgeons, the model serves as an invaluable guide in quickly locating the ureter, thereby preventing inadvertent harm.

However, some gynecologists also advised that the DL model should pay more attention and have higher precision for the boundary of the ureter at the parametrium and the transiliac vessels where the gynaecologists needed to spend more energy to distinguish tissues. Some suggested that it should be practiced in animals first, before testing in clinical practice, and quality control should be carried out. In addition, the appropriate identification of the boundaries of the ureters is also important, as the potential for avoidance of thermal spread and thermal injury during surgery is an important consideration. If it is proven to indeed be reliable, it is expected to help reduce the risk of organ damage during surgery.

In our visualisation approach, the convolutional neural network retains the activation value (feature map) of the last layer, which corresponds to the original image. To gain intuition, visualising the feature map of each layer and observing its value change is common. As the network depth increases, the feature map becomes sparser, indicating the encoding, compression, and transformation of image information into high-level features.

CAM elucidate that the model prioritises identifying the ureter's site and adjacent vasculature. By extracting vascular features, such as direction and texture, it effectively segments the ureter from

surrounding tissues, instilling greater confidence in central areas compared to peripheral boundaries.

It is important to recognise the limitations as well. The model's capacity to differentiate between tissues and organs is subject to the variability of surgical methodologies and environmental factors. Challenges such as fluctuating lighting and bleeding can affect robustness, yet expanding the dataset can mitigate these limitations. CPU-based real-time segmentation is currently unattainable, but with a GPU as the standard hardware, the evolution of AI applications remains unhampered. The present model is susceptible to overfitting due to the limited dataset and is therefore not yet suitable for direct clinical application. Collecting more real-world data and retraining the model is necessary to improve its robustness and accuracy for subsequent experiments.

Operative visual fields can be obstructed, yet peripheral frames often hold crucial contextual information. For instance, pre-bleeding frames can inform the DL model of the ureter's borders and position in the subsequent obscured view. We are poised to design a novel AI that will harness spatial-temporal data from surgical videos, counteracting visual field alterations and thereby bolstering accuracy.

## 5 | CONCLUSIONS

Our DL model operates in real-time to segment the ureter in gynaecological laparoscopic surgery footage, achieving a Dice score of 0.86 and a Hausdorff 95 distance of 22.60, while processing at an expedient rate of just 8 ms per frame. This technological advancement holds the promise of diminishing the incidence of ureteral injuries and augmenting surgical assistance for gynaecologists. Nonetheless, variations across patients and the diverse nature of surgical procedures could potentially affect the model's performance, highlighting the need for an expanded dataset to enhance its adaptability and accuracy.

## AUTHOR CONTRIBUTIONS

Ying Feng and Zhixiang Wang designed the study and wrote the article. Zhen Zhang, Yupeng Deng, Meizhu Xiao, Zhiqiang Zhang, LinXue Qian, and Shuzhen Wang helped to analyse pre-processing of the dataset. Alberto Traverso, Andre Dekker, Chongdong Liu, and Zhenyu Zhang provided administrative support. All authors have read and approved the final manuscript.

## ACKNOWLEDGEMENTS

We really appreciate that the help from these gynaecologists: Fei Li, Cancan Wang, Yiwen Zhang, Peng Guo, Qingyun Guo, Yannan Ma, Hongtao Guo, Dajiang Liu, Rui Liu, Xu Li, Hua Chen, Junyu Shi, Chunyan Xue, Hong Zheng, Bin Tang, Suli He, Zhurong Wang, Ru Sun, Guanmei Chen, Ling Lei, Jing Wang, Yaping Gong, Lijuan Wang, Yingying Hu, Yanli He, Yanhong Lv, Xiao Lv, Guang Yao, Yu Du, Yang Li, Yuan Ma, Haining Li, Huijie Cui, Sufen Cui, Jinjin Zhou, Yujie Sun, Xinchun Xiao, Xiaoyan Li, Bin Zhu, Xiaofeng Zhao, Xuehan Bi, Chang



Liu, Dan Liu, Yan Li, Yonghui Ding, Qing Wang, Hongyan Gao, Zhihui Cai, Ke Yu, Yunfang Zhu, Guimeng He, Yahong Liu and Dandan Zhang, who are the members of Chinese Obstetricians and Gynecologist Association (COGA). We thank the Chinese Scholarship Council (CSC) for their financial support for studying abroad.

### CONFLICT OF INTEREST STATEMENT

The authors declare that they have no competing interests.

### DATA AVAILABILITY STATEMENT

The data are available from the corresponding author on reasonable request.

### ORCID

Zhixiang Wang  <https://orcid.org/0000-0002-4778-7539>

### REFERENCES

- Aarts JW, Nieboer TE, Johnson N, et al. Surgical approach to hysterectomy for benign gynaecological disease. *Cochrane Database Syst Rev*. 2015;8:CD003677. <https://doi.org/10.1002/14651858.CD003677.pub5>
- King CR, Giles D. Total laparoscopic hysterectomy and laparoscopic-assisted vaginal hysterectomy. *Obstet Gynecol Clin North Am*. 2016;43(3):463-478. <https://doi.org/10.1016/j.ogc.2016.04.005>
- Desai VB, Wright JD, Lin H, et al. Laparoscopic hysterectomy route, resource use, and outcomes: change after power morcellation warning. *Obstet Gynecol*. 2019;134(2):227-238. <https://doi.org/10.1097/AOG.0000000000003375>
- Boosz A, Haerberle L, Renner SP, et al. Comparison of reoperation rates, perioperative outcomes in women with endometrial cancer when the standard of care shifts from open surgery to laparoscopy. *Arch Gynecol Obstet*. 2014;290(6):1215-1220. <https://doi.org/10.1007/s00404-014-3347-9>
- Yabuki Y, Asamoto A, Hoshiba T, Nishimoto H, Nishikawa Y, Nakajima T. Radical hysterectomy: an anatomic evaluation of parametrical dissection. *Gynecol Oncol*. 2000;77(1):155-163. <https://doi.org/10.1006/gyno.1999.5723>
- Yoo S, Terai Y, Tanaka T, et al. Role of the two-point pull-up technique for treating the uterine arteries during radical hysterectomy and trachelectomy. *Eur J Obstet Gynecol Reprod Biol*. 2013;170(2):544-549. <https://doi.org/10.1016/j.ejogrb.2013.08.001>
- Kim TN, Kim JH, Oh CK, Lee W, Nam JK, Lee KS. Three different laparoscopic techniques for the management of iatrogenic ureteral injury: a multi-institutional study with medium-term outcomes. *Asian J Surg*. 2021;44(7):964-968. <https://doi.org/10.1016/j.asjsur.2021.01.027>
- Burks FN, Santucci RA. Management of iatrogenic ureteral injury. *Ther Adv Urol*. 2014;6(3):115-124. <https://doi.org/10.1177/1756287214526767>
- Likic IS, Kadija S, Ladjovic NG, et al. Analysis of urologic complications after radical hysterectomy. *Am J Obstet Gynecol*. 2008;199(6):644.e1-644.e3. <https://doi.org/10.1016/j.ajog.2008.06.034>
- Rob L, Skapa P, Robova H. Fertility-sparing surgery in patients with cervical cancer. *Lancet Oncol*. 2011;12(2):192-200. [https://doi.org/10.1016/S1470-2045\(10\)70084-X](https://doi.org/10.1016/S1470-2045(10)70084-X)
- Gilmour DT, Das S, Flowerdew G. Rates of urinary tract injury from gynecologic surgery and the role of intraoperative cystoscopy. *Obstet Gynecol*. 2006;107(6):1366-1372. <https://doi.org/10.1097/01.aog.0000220500.83528.6e>
- Fujii S, Takakura K, Matsumura N, et al. Precise anatomy of the vesico-uterine ligament for radical hysterectomy. *Gynecol Oncol*. 2007;104(1):186-191. <https://doi.org/10.1016/j.ygyno.2006.07.041>
- Kobayashi E, Iwamiya T, Isobe M, Miyake T, Shiki Y, Yamasaki M. A novel technique for the management of the vesicouterine ligament during radical hysterectomy. *Gynecol Oncol*. 2009;115(1):56-59. <https://doi.org/10.1016/j.ygyno.2009.06.034>
- Ward TM, Hashimoto DA, Ban Y, et al. Automated operative phase identification in peroral endoscopic myotomy. *Surg Endosc*. 2021;35(7):4008-4015. <https://doi.org/10.1007/s00464-020-07833-9>
- Maas AL, Hannun AY, Ng AY. Rectifier nonlinearities improve neural network acoustic models. In: *Proc. ICML*. Citeseer; 2013; Vol 1:3.
- Harangi B, Hajdu A, Lampe R, Torok P. Recognizing ureter and uterine artery in endoscopic images using a convolutional neural network. In: *IEEE 30th International Symposium on Computer-Based Medical Systems (CBMS)*. IEEE; 2017:726-727.
- Zhou B, Khosla A, Lapedriza A, Oliva A, Torralba A. Learning deep features for discriminative localization. In: *Proceedings of the IEEE conference on computer vision and pattern recognition*; 2016:2921-2929.
- Morita S, Tabuchi H, Masumoto H, Yamauchi T, Kamiura N. Real-time extraction of important surgical phases in cataract surgery videos. *Sci Rep*. 2019;9(1):16590. <https://doi.org/10.1038/s41598-019-53091-8>
- Cardenas CE, Yang J, Anderson BM, Court LE, Brock KB. Advances in auto-segmentation. *Seminars Radiat Oncol*. 2019;29(3):185-197. <https://doi.org/10.1016/j.semradonc.2019.02.001>
- Yabuki Y, Asamoto A, Hoshiba T, Nishimoto H, Kitamura S. Dissection of the cardinal ligament in radical hysterectomy for cervical cancer with emphasis on the lateral ligament. *Am J Obstet Gynecol*. 1991;164(1 Pt 1):7-14. [https://doi.org/10.1016/0002-9378\(91\)90614-w](https://doi.org/10.1016/0002-9378(91)90614-w)
- Gueli Alletti S, Restaino S, Finelli A, et al. Step by step total laparoscopic hysterectomy with uterine arteries ligation at the origin. *J Minim Invasive Gynecol*. 2020;27(1):22-23. <https://doi.org/10.1016/j.jmig.2019.06.001>
- Wu M, Xie W, Shi X, Shao P, Shi Z. Real-time drone detection using deep learning approach. In: *Machine Learning and Intelligent Communications*. Lecture Notes of the Institute for Computer Sciences, Social Informatics and Telecommunications Engineering; 2018:22-32. [https://doi.org/10.1007/978-3-030-00557-3\\_3](https://doi.org/10.1007/978-3-030-00557-3_3)
- Niamh Curtin DW, Cahill R, Sarkar A, et al. Dual color imaging from a single BF2-azadipyrrromethene fluorophore demonstrated in vivo for lymph node identification. *Int J Med Sci*. 2021;18(7):1541-1553. <https://doi.org/10.7150/ijms.52816>

### SUPPORTING INFORMATION

Additional supporting information can be found online in the Supporting Information section at the end of this article.

**How to cite this article:** Wang Z, Liu C, Zhang Z, et al. Real-time auto-segmentation of the ureter in video sequences of gynaecological laparoscopic surgery. *Int J Med Robot*. 2024; e2604. <https://doi.org/10.1002/rcs.2604>